Topology Optimization with Shape Preserving Design

*** ZHU Ji-Hong*, LI Yu, ZHANG Wei-Hong**

[1] Engineering Simulation and Aerospace Computing (ESAC), The Key Laboratory of Contemporary Design and Integrated Manufacturing Technology, Northwestern Polytechnical University, Xi'an, P.R. China

*Corresponding author: jh.zhu@nwpu.edu.cn

Abstract

This paper is to present an extended shape preserving topology optimization formulation aiming at preserving specific local structural domain configuration. By introducing Artificial Week Elements (AWE) established with respect to shape preserving control points, we constrain its elastic strain energy to suppress the warping deformation. Compared with the existing global compliance topology optimization, this formulation acts as a control of local compliance of the structure. Numerical results have shown how the strain energy constraint related to AWE influences the optimized solution, especially the effect of the upper limit of the constraint. Comparative studies have evidently shown that the effect of shape preserving can be successfully achieved. Possible structural distortions are also illustrated in order to have an in-depth understanding of the design mechanism.

Keywords: Topology Optimization, Shape Preserving, Artificial Weak Elements, Warping Deformation, Local Strain Energy

Introduction

Topology optimization method has been developed as one of the most effective techniques in saving structural weight and improving multidisciplinary performances. Recent advances of topology optimization techniques have been summarized by excellent literature surveys such as Guo and Cheng (2010), Sigmund and Maute (2013), Deaton and Grandhi (2014).

Meanwhile, different topology optimization formulations were also presented to obtain required structural deformation patterns. In these literatures, constraints on a single or multiple nodal displacements were normally issued. For example, in the works of Liu et al. (2008), warping deformation of beam cross-section was considered in a new anisotropic beam theory as well as in topology optimization. Rong and Yi (2010) designed the multi-points displacements using a newly developed phase transferring method. Typically, in the works of Qiao and Liu (2012), a geometric average displacement function integrating the deformation field, which was similar to a P-norm scheme, was proposed to minimize the structural maximum deformation. In this way, the magnitudes of different nodal displacements were controlled to form a better deformation. Other displacement designs can be found mostly in topology optimization of compliant mechanisms (see e.g. Wang et al. 2005, Stanford et al. 2012 and 2013).

However, constraints on the magnitudes of nodal displacements might not appropriate in many complicated engineering cases searching better structural deformation behaviors. For example, challenges of suppressing structural local warping deformation to maintain structural coordinative displacements are always faced during the aircraft structure design, manufacturing and assembling (Niu 1988, Barrett 1992, Wang 2000), which are considered as shape preserving design. Key difficulties lies in that the popularly used global compliance and nodal displacements in topology optimization cannot effectively describe and suppress the local warping deformation.

Therefore, this paper proposes to implement multi-point shape preserving constraints in an extended topology optimization formulations by introducing strain energy based quantitative approach describing warping deformation magnitudes in shape preserving domain.

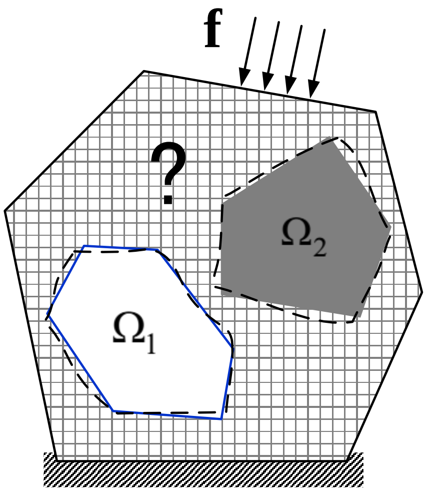

Figure 1. An illustrative structure system for shape-preserving design problem (Dashed lines indicates probable deformation for the loaded structure)

Multi-Point Shape Preserving Design

Local domains are concerned for shape preserving as shown in **Figure** 1. They may be void (e.g. a structural opening for process, feature or maintenance) or solid (e.g. a structural branch or a component), or even hybrid (e.g. parts or equipment). When it comes to situations like structural installing, connecting and assembling problems mostly based on the point locations, it is essential to have proper design of multi-point shape preserving i.e. coordinative displacement of control points. Therefore, we propose to define Artificial Week Elements (AWE) established with respect to the above mentioned control points. The local strain energies related to AWE are considered as additional constraints to suppressing the warping deformation.

Structural Deformation

The nodal displacement vector $\mathbf{u}_{\Omega}$ of the local domain Ωis composed by two components of rigid displacement vector $\mathbf{u}_{\Omega\mathrm{R}}$ and warping deformation vector $\mathbf{u}_{\Omega\mathrm{W}}$, i.e.

$$\mathbf{u}_{\Omega} = \mathbf{u}_{\Omega\mathrm{R}} + \mathbf{u}_{\Omega\mathrm{W}} \tag{1}$$

To achieve the structural shape preserving design necessitates suppression of the warping deformation. As a result, local strain energy is used to describe and constrain warping deformation quantitatively here. It is expressed as

$$C_{\Omega} = \frac{1}{2}\mathbf{u}_{\Omega}^{\mathrm{T}}\mathbf{K}_{\Omega}\mathbf{u}_{\Omega} \tag{2}$$

where $\mathbf{K}_{\Omega}$ is the local domain stiffness matrix.

Since no strain energy produced by rigid displacement, the above expression can be written as

$$C_{\Omega} = \frac{1}{2}\mathbf{u}_{\Omega\mathrm{W}}^{\mathrm{T}}\mathbf{K}_{\Omega}\mathbf{u}_{\Omega\mathrm{W}} \tag{3}$$

Theoretically, there would be no elastic warping deformation but only rigid body movement under a perfect shape preserving design where the local strain energy is 0. But practically the perfect effect is unobtainable. The constraint is given by a minor upper bound above zero, i.e. ε. The shape preserving design achieves a fairly well effect in permissible tolerance when the strain energy value satisfies

$$C_{\Omega} \le \varepsilon \tag{4}$$

Artificial Week Elements

However, the shape preserving design will degenerate into an all-domain shape preserving when the elastic strain energy of the local domain is directly defined as a constraint function, which is an over constraint issue compared with multi-point shape preserving design. In this paper, Artificial Weak Elements (AWE) is proposed and established with respect to the shape preserving control points. The AWE nodal Degrees of Freedom (DOFs) are coupled to those of the control points. By calculating the AWE strain energy, the warping deformation of these multiple points can be measured.

Besides, to ensure the precision of structural analysis, the stiffness of additional AWE should be weak enough not to influence the structural mechanical properties. In this paper, the Poisson's ratio is set to a general value 0.3, and the elastic modulus is set to 1 Pa, which is much smaller than regular material.

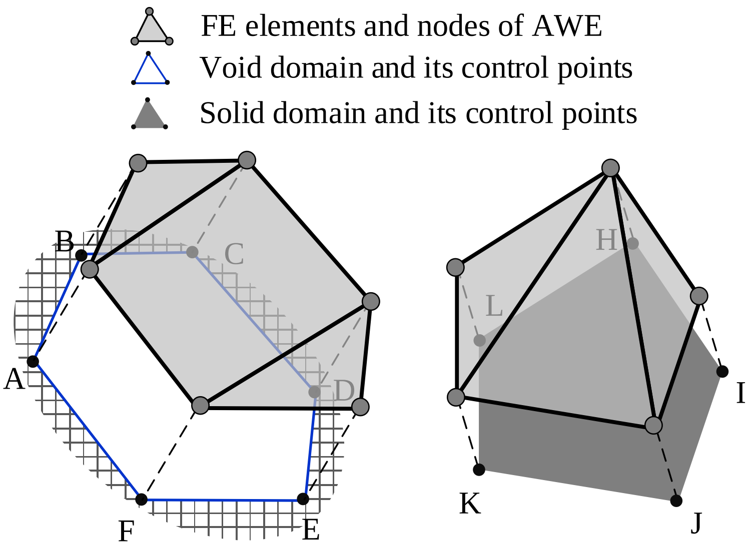

Figure 2. The definition of AWE

For the shape preserving design illustrated in **Figure** 1, AWE can be established as shown in **Figure** 2. The outline boundaries contain 11 control points, i.e. points A to L. Then 6 additional weak elements are created with the 11 points respectively. When the total structure is loaded, the AWE deform along with the control points. At this point, the shape preserving constraint can be defined as AWE strain energy constraint, i.e.

$$C_{\mathrm{AWE}} \le \varepsilon \tag{5}$$

Therefore, the topology optimization with shape preserving design is formulated as

$$\begin{aligned} \text{find:} \quad & \boldsymbol{\eta} = (\eta_1, \eta_2, \ldots, \eta_i, \ldots, \eta_n) \\ \text{min:} \quad & C = \frac{1}{2}\mathbf{u}^{\mathrm{T}}\mathbf{K}\mathbf{u} \\ \text{s.t.:} \quad & \mathbf{f} = \mathbf{K}\mathbf{u};\ V \le V_0;\ C_{\mathrm{AWE}} \le \varepsilon \end{aligned} \tag{6}$$

In the above formulations, $\boldsymbol{\eta}$ is the vector of pseudo-density design variables, whose items' values vary from 0 to 1 describing material distribution in design domain. SIMP interpolation model (see Bendsøe and Sigmund 1999, Rozvany 2001) is used here with the penalty factor equals to 3. The global strain energy C is minimized as the object function. $\mathbf{K}$ is the global stiffness matrix. V is the material volume and V_0 is its upper bound. ε is a given minor upper bound, whose value is relevant to specific structure and problem.

Sensitivity Analyses on Shape Preserving Constraint

The design sensitivity of the object function, i.e. the global strain energy with respect to the pseudo-densities is easily obtained and can be found in many references dealing with the topology optimization problems (e.g. Sigmund 2001), which will not be provided here.

We mainly concern the sensitivity of the constrained AWE strain energy. It can be expressed as

$$C_{\mathrm{AWE}} = \frac{1}{2}\mathbf{u}_{\mathrm{AWE}}^{\mathrm{T}}\mathbf{K}_{\mathrm{AWE}}\mathbf{u}_{\mathrm{AWE}} \tag{7}$$

$\mathbf{u}_{\mathrm{AWE}}$ is the displacement vector of control points, i.e. nodes of AWE. $\mathbf{K}_{\mathrm{AWE}}$ is the stiffness matrix of AWE

Derivative of the AWE strain energy is written as

$$\begin{aligned}\frac{\partial C_{\mathrm{AWE}}}{\partial \eta_i} &= \frac{1}{2}\mathbf{u}_{\mathrm{AWE}}^{\mathrm{T}}\frac{\partial \mathbf{K}_{\mathrm{AWE}}}{\partial \eta_i}\mathbf{u}_{\mathrm{AWE}} + \mathbf{u}_{\mathrm{AWE}}^{\mathrm{T}}\mathbf{K}_{\mathrm{AWE}}\frac{\partial \mathbf{u}_{\mathrm{AWE}}}{\partial \eta_i} \\ &= \mathbf{u}_{\mathrm{AWE}}^{\mathrm{T}}\mathbf{K}_{\mathrm{AWE}}\frac{\partial \mathbf{u}_{\mathrm{AWE}}}{\partial \eta_i}\end{aligned} \tag{8}$$

where the stiffness matrix of AWE is independent from topology design variables η_i.

Here we define $\mathbf{u}_{\mathrm{AWE}} = \mathbf{T}_{\mathrm{AWE}}\mathbf{u}$, where $\mathbf{T}_{\mathrm{AWE}}$ is a constant matrix which converts the global displacement vector $\mathbf{u}$ to the local one $\mathbf{u}_{\mathrm{AWE}}$. Following the derivative of the equilibrium equation, we further have

$$\frac{\partial \mathbf{u}_{\mathrm{AWE}}}{\partial \eta_i} = \mathbf{T}_{\mathrm{AWE}}\frac{\partial \mathbf{u}}{\partial \eta_i} = \mathbf{T}_{\mathrm{AWE}}\mathbf{K}^{-1}\left(\frac{\partial \mathbf{f}}{\partial \eta_i} - \frac{\partial \mathbf{K}}{\partial \eta_i}\mathbf{u}\right) \tag{9}$$

Substituting the above equation into equation (8), it turns into

$$\begin{aligned}\frac{\partial C_{\mathrm{AWE}}}{\partial \eta_i} &= \mathbf{u}_{\mathrm{AWE}}^{\mathrm{T}}\mathbf{K}_{\mathrm{AWE}}\mathbf{T}_{\mathrm{AWE}}\mathbf{K}^{-1}\left(\frac{\partial \mathbf{f}}{\partial \eta_i} - \frac{\partial \mathbf{K}}{\partial \eta_i}\mathbf{u}\right) \\ &= \left(\boldsymbol{\lambda}^*\right)^{\mathrm{T}}\mathbf{K}^{-1}\left(\frac{\partial \mathbf{f}}{\partial \eta_i} - \frac{\partial \mathbf{K}}{\partial \eta_i}\mathbf{u}\right)\end{aligned} \tag{10}$$

where we formulated a new vector $\boldsymbol{\lambda}^*$ calculated from the AWE displacements vector, stiffness matrix and the constant matrix, i.e. $\boldsymbol{\lambda}^* = \mathbf{u}_{\mathrm{AWE}}^{\mathrm{T}}\mathbf{K}_{\mathrm{AWE}}\mathbf{T}_{\mathrm{AWE}}$.

It is informed that $\boldsymbol{\lambda}^*$ is a column vector whose dimension is equal to total DOFs. After one additional finite element analysis by applying $\boldsymbol{\lambda}^*$ as an artificial load vector on the structure, we have

$$\begin{aligned}&\boldsymbol{\lambda}^* = \mathbf{K}\mathbf{u}^* \\ &\left(\boldsymbol{\lambda}^*\right)^{\mathrm{T}}\mathbf{K}^{-1} = \left(\mathbf{u}^*\right)^{\mathrm{T}}\end{aligned} \tag{11}$$

Then the derivative of local elastic strain energy can be expressed as

$$\frac{\partial C_{\mathrm{AWE}}}{\partial \eta_i} = \left(\mathbf{u}^*\right)^{\mathrm{T}}\left(\frac{\partial \mathbf{f}}{\partial \eta_i} - \frac{\partial \mathbf{K}}{\partial \eta_i}\mathbf{u}\right) \tag{12}$$

The derivatives of the load vector and the stiffness matrix with respect to the pseudo-densities are easily obtained according to the SIMP interpolation model used in this paper. Typically, in the case of design independent loads, the derivative of the load vector will be zero, i.e. $\dfrac{\partial \mathbf{f}}{\partial \eta_i} = 0$.

Numerical Examples of Shape Preserving Design

L-shape Beam

Here we optimize an L-shape beam aimed at preserving the cutout configuration as shown in **Figure** 3. The top boundary is fixed and a single-point force of 100N is applied on the right corner. A frame with a particular non-design width is assigned around the cutout. Shape preserving control points are the four corners of the frame and the corresponding AWE is one quadrangle weak element linked to the control points A to D. Under the constraint of 40% material volume fraction, standard topology optimization design merely maximizing the overall structural stiffness is shown in **Figure** 4(a). Afterwards, without any other conditions changed, shape preserving design is shown in **Figure** 4(b), where ε equal to 2×10^{-15}J. The optimized strain energies of global structure, shape preserving frame domain and the AWE are listed in Table 1. The strain energy of AWE is decreased from 8.58×10^{-15}J to 2.00×10^{-15}J under the effect of shape preserving constraint, while the loss of global structure stiffness is less than 6%.

To have an obvious view of the shape preserving effect, a comparison of enlarged deformation of the frame is presented in **Figure** 5. The standard design generates a large warping deformation. On the contrary, the shape preserving design achieves a better deformation behavior where the frame corners' displacements was coordinated.

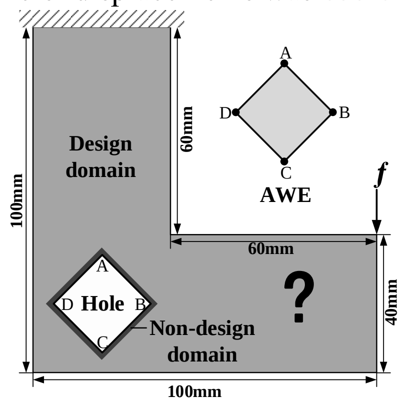

Figure 3. An L-shape beam with a quadrate cutout and its AWE

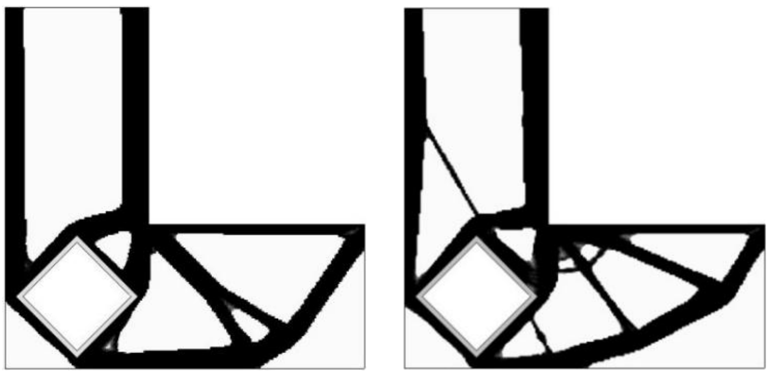

(a) (b)

(a) Standard topology optimization
(b) Shape preserving design
Figure 4. Comparison of the L-shape beam designs

Table 1. Comparisons of strain energies of the optimized L-shape beam

Strain Energy	Global structure	Frame around the cutout	AWE
Standard topology optimization	1.17×10^{-4}J	8.57×10^{-6}J	8.58×10^{-15}J
Shape preserving design	1.24×10^{-4}J	4.21×10^{-6}J	2.00×10^{-15}J

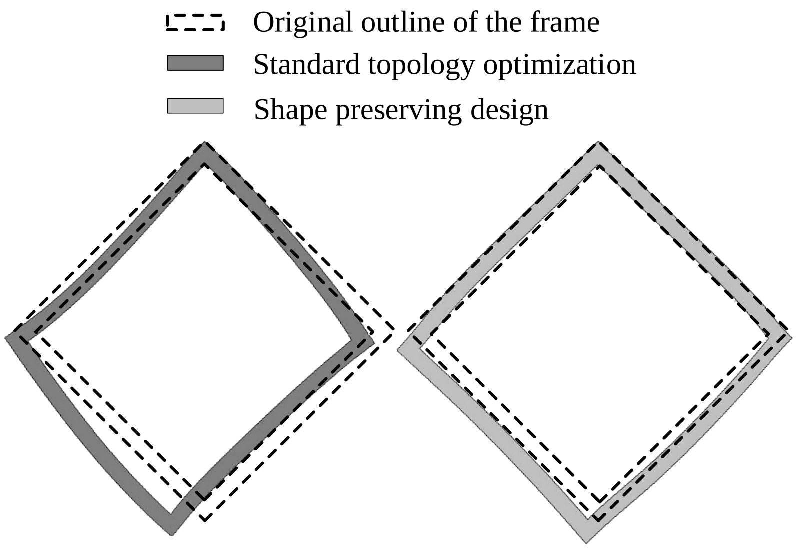

Figure 5. Comparison of enlarged deformations of the frame around the hole in optimized designs (Amplification factor 1.5×10^7)

Furthermore, the optimized results with different material volume are presented in **Figure** 6. C and C_{AWE} represent the optimized strain energy of global structure and AWE in standard topology design. C^* and C^*_{AWE} represent the optimized strain energy of global structure and AWE in shape preserving design.

For the standard topology optimization, the structure material is always distributed on the optimal load carrying path as a result of seeking maximum stiffness of global structure. Consequently, the standard design results always have smaller global strain energies. In shape preserving design, the local strain energy of AWE is much lower than the standard one with a little sacrifice on its global stiffness to satisfy local shape preserving constraint. This paradox between shape preserving constraint and global strain energy indicates that the final optimized design will be a compromise between global stiffness and local deformation.

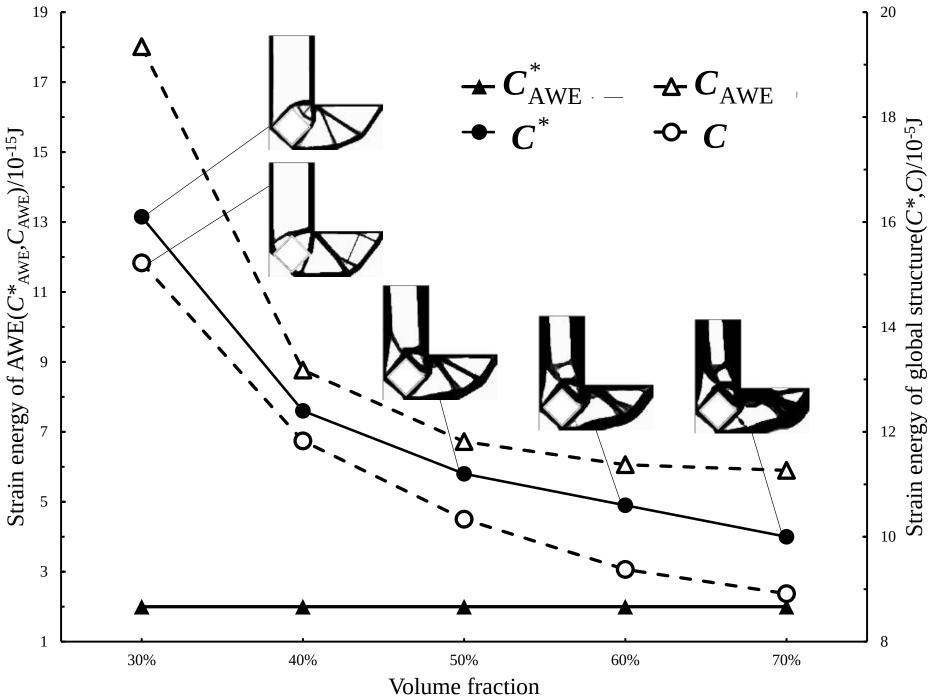

Figure 6. Optimized designs versus different volume fraction and their strain energy

Distortion of Load Carrying Path

For in-depth understanding of the paradox, further discussions on the upper bound of shape preserving constraint and its influence on the structural optimization design are discussed here.

Taking the L-shape beam design for example, we obtain optimized design in **Figure** 7 in turn via changing the value of ε with the rest conditions keeping identical. The optimized configurations change gradually as the value of ε decreases. When the shape preserving constraint is so strong, the structural load carrying path will be distortional (e.g. 11^{th} and 12^{th} result) with unsatisfied large sacrifice of global stiffness. In these cases, regular structural design cannot meet the requirement of shape preserving constraints. The topology optimization is forced to separate the shape preserving domain from the load carrying path to obtain an approximate rigid deformation. Such result is mathematically reasonable but loses actual physical significance and engineering value in optimization design.

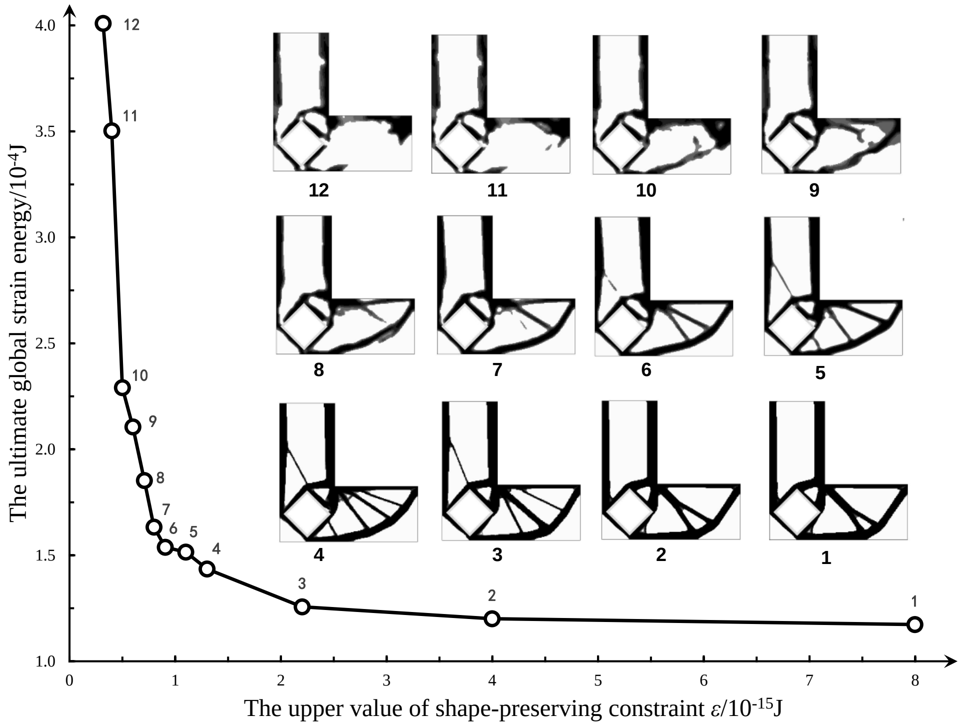

Figure 7. The global strain energy and corresponding optimized design results versus different constraint values of ε

Accordingly, the upper bound of shape preserving constraint should be appropriately chosen to avoid phenomena of load carrying path distortion. Meanwhile, researchers are not only to solve a mathematical model but also to account for more practical problems into consideration, which is one of the key difficulties in optimization design for engineering structures.

Shape Preserving Design for Windshields

Consider now an airframe shown in **Figure** 8. The front fuselage is connected to the center one at its rear side. The whole fuselage bears aerodynamic loads. Warping deformations of windshields need to be avoided not to cause the glasses fracture. Here, AWE is defined as illustrated in **Figure** 8. The control points of each windshield contain four corners and four midpoints of the boundaries as well. With the airframe's layout as topology optimization design subject, two material distribution results of skin reinforcement from standard design and shape preserving design are presented in **Figure** 9. The value of the shape preserving constraint ε is set as 0.02J.

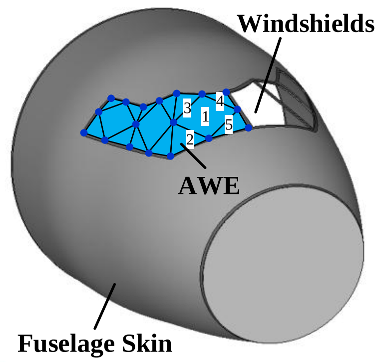

Figure 8. Illustration of shape preserving design of windshields

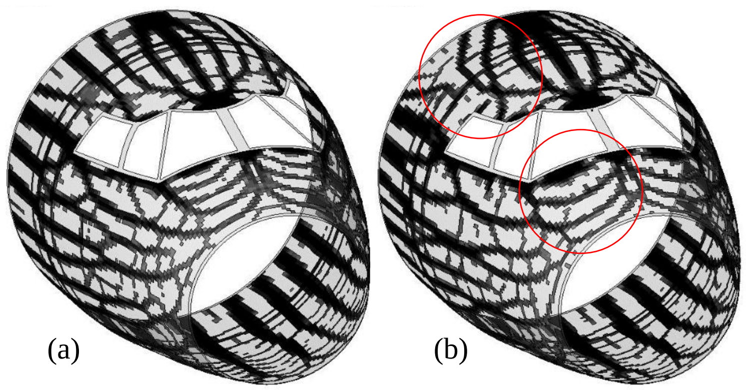

(a) Standard topology optimization design
(b) Shape preserving design

Figure 9. Comparison of material distributions of skin reinforcement

Referring to the optimized designs with the same volume fractions in **Figure** 9, we can distinguish that the material distributed around the windshields increases in the shape preserving design. Therefore, the prescribed local domain is strengthened and the warping deformation is suppressed. Additionally in the weak loaded area between windshields and center fuselage, the shape preserving design modifies the load carrying path to offset the warping deformation in the windshields. The detailed data of shape preserving design and standard stiffness design is listed and compared in Table 2. Although there is a 5% sacrifice on the stiffness of global structure, the shape preserving design has improved the effect of shape preserving for 4 times better than the standard one. Thus, the effectiveness of shape preserving topology optimization design is further demonstrated, which possesses a good perspective in practical structure design applications.

Table 2. Comparisons of strain energies of optimized designs

Strain energy	The whole fuselage	The AWE of windshields
Standard optimization design	6893 J	0.092 J
Shape-preserving optimization design	7263 J	0.020 J

Conclusions

We proposed an extended structural topology optimization method with multi-point shape preserving constraint in this paper. The shape preserving constraint of local domain is constructed by the strain energy of Artificial Weak Elements (AWE). Compared with the standard topology optimization design maximizing structural stiffness, this formulation have evidently shown that the coordination of multi-point displacements and the effect of shape preserving can be successfully achieved. Further numerical results are analyzed to show the influence of shape preserving constraint on the optimized design pattern and the entire performance of structure. Besides, the design distortion due to improper definition of the shape preserving constraint is revealed and studied in this paper.

Acknowledgment

This work is supported by National Natural Science Foundation of China (90916027, 51275424, 11172236), 973 Program (2011CB610304), the 111 Project (B07050), NPU Foundation for Fundamental Research (JC20120229).

References

Barrett R. T. (1992) Fastener Design Manual. *NASA Reference Publication* 1228

Bendsøe M. P. Sigmund O. (1999) Material interpolation schemes in topology optimization. *Archive of Applied Mechanics*, **69(9-10)**:635~654.

Deaton J. D., Grandhi R. V. (2014) A survey of structural and multidisciplinary continuum topology optimization: post 2000. *Structural and Multidisciplinary Optimization* **49**:1-38

Guo X., Cheng G. D. (2010) Recent development in structural design and optimization. *Acta Mechanica Sinica* **26**:807-823

Liu S., An X., Jia H. (2008) Topology optimization of beam cross-section considering warping deformation. *Structural and Multidisciplinary Optimization* **35**:403-411

Niu M. C. Y. (1988) Airframe Structural Design: Practical Design Information and Data on Aircraft Structures, *Technical Book Co*

Qiao H. T., Liu S. T. (2013) Topology optimization by minimizing the geometric average displacement. *Engineering Optimization* **45**:1-18

Rong J., Yi J. (2010) A structural topological optimization method for multi-displacement constraints and any initial topology configuration. *Acta Mechanica Sinica* **26**:735-744

Rozvany G. I. N. (2001) Aims, scope, methods, history and unified terminology of computer-aided topology optimization in structural mechanics. *Structural and Multidisciplinary Optimization*, **21(2)**: 90-108.

Sigmund O., Maute K. (2013) Topology optimization approaches. *Structural and Multidisciplinary Optimization* **48**:1031-1055

Sigmund O. (2001) A 99 line topology optimization code written in Matlab[J]. *Structural and Multidisciplinary Optimization*, **21(2)**: 120-127.

Stanford B., Beran P. (2012) Optimal Compliant Flapping Mechanism Topologies With Multiple Load Cases. *Journal Of Mechanical Design* 134

Stanford B., Beran P., Kobayashi M. (2013) Simultaneous topology optimization of membrane wings and their compliant flapping mechanisms. *Aiaa J* **51**:1431-1441

Wang B. Z. (2000) Aircraft Design Manual 10: Structural Design, *Aviation Industry Press*, Beijing

Wang M. Y. , Chen S. K. , Wang X. M., Mel Y. L. (2005) Design of multimaterial compliant mechanisms using level-set methods. *J Mech Design* **127**:941-956